Materials Science and Engineering, 31 (1977) 107 - 114

Intralayer Crystal Structure and Order–Disorder Transformations of Graphite Intercalation Compounds using Electron Diffraction Techniques*,**

D. D. L. CHUNG***, G. DRESSELHAUS† and M. S. DRESSELHAUS††
Massachusetts Institute of Technology, Cambridge, MA 02139 (U.S.A.)

SUMMARY

We have used electron diffraction through the *c*-face to study the intercalate ordering of graphite–alkali metals (K, Rb, Cs) and graphite–halogens (Br_2, IBr, ICl). Order–disorder transformations for the in-plane structure of alkali metal and halogen intercalates have been observed by the vanishing of all superlattice diffraction spots as the sample temperature is raised. Variations of the electron diffraction patterns and of the order–disorder transformation temperatures with the intercalate species are reported. Compounds of various concentrations have been investigated, including the stage 1 graphite–alkali metals. Results obtained here are compared with structural information obtained by other techniques and by previous workers. The patterns for graphite–halogens are much more complicated than those for graphite–alkali metals. Of significance is the observation that the superlattice patterns are relatively insensitive to the intercalate concentration for compounds more dilute than stage 2 and are similar for lamellar and residue compounds. Additional superlattice patterns are observed in graphite–Br_2 below 194 °C and are similar in appearance to charge-density wave superlattice patterns reported for 2H-$TaSe_2$.

RESUME

Nous avons utilisé la diffraction électronique à travers la face *c* pour étudier la matière insérée et ordonnée dans le plan des composés graphite–métaux alcalins (K, Rb, Cs) et des graphite-halogènes (Br_2, IBr, ICl). Les transformations d'ordre–désordre pour les structures dans le plan des intercalates ont été observées par la disparition de toutes les taches de diffraction du super-réseau lorsque la température de l'échantillon est augmentée. Les modèles de diffraction électronique et les températures de transformation ordre–désordre varient avec les substances insérées et leur concentrations. Les composés lamellaires et résiduels de différentes concentrations ont été bien étudiés, y compris le stade 1 des métaux alcalins–graphite. Les modèles pour les halogènes–graphite sont beaucoup plus compliqués que ceux pour les métaux alcalins–graphite. Ils sont aussi compatibles avec nos résultats de diffusion-Raman qui fournissent une preuve très claire de l'identité moléculaire de l'halogène intercallé. Les modèles de diffraction de super-réseau devraient donner des informations sur l'ordre dans le plan. Les modèles de super-réseaux sont relativement insensibles à la concentration de la matière insérée pour des composés plus dilués que le stade 2. On trouve aussi les mêmes modèles de super-réseaux pour des composés lamellaires très dilués et pour des composés résiduels de concentration aussi faible que 0,3 mole% Br_2. Ces observations montrent que l'ordre dans le

*Work supported by United States NSF Grant #DMR 76-12226.

**This paper is based on a thesis submitted by D.D. L.C. in partial fulfillment for the Ph. D. degree in the Department of Materials Science and Engineering, Massachusetts Institute of Technology, Cambridge, MA, U.S.A., 1977 (unpublished).

***Department of Materials Science and Engineering and Center for Materials Science and Engineering.

†Francis Bitter National Magnet Laboratory, supported by the United States National Science Foundation.

††Department of Electrical Engineering and Computer Science, and Center for Materials Science and Engineering.

plan est conservé pour de très faibles dilutions, et même pour les composés résiduels.

INTRODUCTION

The vast majority of experimental studies on graphite intercalation compounds has been made on samples based on a highly-oriented pyrolytic graphite host material [1]. Because the in-plane crystallite dimension in this material is ~1 μm [2], by using diffraction areas of ~1 μm in diameter, the electron diffraction technique can provide information from a single crystallite. Thus, this technique is especially appropriate for studies of the crystal structure of graphite intercalation compounds.

Using electron diffraction techniques [2], we have investigated the in-plane crystal structure and the associated intralayer order–disorder transformations in graphite–alkali metal and graphite–halogen intercalation compounds in the temperature range $77 < T < 500$ K. Although diffraction studies have been carried out previously [3 - 9], no direct observation has been made of the disappearance of a superlattice structure as the temperature is increased. In the present work, attention is also given to the effect of intercalate concentration on the intralayer structure. Electron diffraction patterns for stage 1 and higher stage alkali metal compounds are shown. These results are compared with previous electron diffraction studies of alkali metal compounds [9]. Attempts to determine the intralayer ordering by electron diffraction in molecular intercalation compounds have not led to a complete determination because of the complexity of the superlattice structure: graphite–Br_2 [10], graphite–ICl [11], graphite–$FeCl_3$ [12], graphite–$MoCl_5$ [13]. The results reported here for the graphite–halogen compounds suffer from this same difficulty.

For graphite–bromine, in addition to the complex superlattice patterns associated with intralayer ordering, much simpler superlattice diffraction patterns are observed and are tentatively identified with charge-density waves.

The crystal structure of graphite intercalation compounds involves both the interlayer and intralayer ordering. The interlayer ordering has been studied by many workers by means of X-ray diffraction [3 - 6, 14]. However, considerably less attention has been given to studies of the intralayer ordering [3, 8, 11], which is the main focus of this paper. The intercalate ordering in graphite intercalation compounds is temperature-dependent, with order–disorder transformations due to interlayer ordering expected at a higher temperature, T_u, than the intralayer ordering temperature T_l. At temperatures $T_l < T < T_u$ the carbon and intercalate layers are well ordered along the c-axis, but the intercalate is disordered within each intercalate layer. For $T < T_u$, the compound may become a disordered solid solution or become unstable thermodynamically. For $T < T_l$, 3-dimensional ordering is established. No order–disorder transformations have been reported for stage 1 alkali metal compounds. However, for the stage 2 alkali metal compounds, changes of observed X-ray diffraction patterns have been interpreted in terms of an intralayer order–disorder transformation [7, 8] in $C_{24}K$ at −175 °C, $C_{24}Rb$ at −114 °C and $C_{24}Cs$ at −110 °C. Order–disorder transformations have also been studied in terms of anomalies in the temperature dependence of the electronic transport parameters. Discontinuities in the temperature dependence of the electrical resistivity have been interpreted in terms of an order–disorder transformation at −20 °C for graphite nitrate [15, 16]. Preliminary results have also been reported on anomalies in the temperature dependence of the electrical resistivity of graphite–alkali metal compounds [17].

EXPERIMENTAL

Electron diffraction measurements through the c-face were made with a Philips EM300 transmission electron microscope using electrons of 80 or 100 kV and a diffraction diameter of ~1 μm on the sample. The electron beam is along the c-axis of the sample, so that the diffraction pattern obtained corresponds to the (001) reciprocal lattice plane. Therefore, this technique is most sensitive to the intralayer ordering. For electron transmission, the specimen thickness has to be $\lesssim 1\,000$ Å. For each specimen, diffraction patterns were obtained at a number of different locations

on the sample. The specimens were prepared by cleavage from the bulk compound, which was based on highly-oriented pyrolytic graphite. For the graphite–alkali metals, which are air-sensitive, specimen preparation and mounting were carried out under nitrogen atmosphere in a glove bag. The specimens were quickly cooled to liquid nitrogen temperature after loading into the electron microscope in order to minimize intercalate desorption. The specimen temperature could be varied from liquid nitrogen temperature to ~750 °C by means of a cold stage and a hot stage on the electron diffraction unit.

RESULTS AND DISCUSSION

We have studied variations with temperature and intercalate concentration of the electron diffraction patterns for lamellar and residue compounds of the graphite–halogens and lamellar graphite–alkali metals [2]. The same (001) electron diffraction pattern is found for our stage 1 samples of C_8K (Fig. 1(b)) and C_8Cs (Fig. 1(c)), but differing from that observed in pristine graphite (Fig. 1(a)). These stage 1 graphite–alkali metal electron diffraction patterns correspond to the reciprocal and real space in-plane unit cells shown in Fig. 2. This in-plane structure is consistent with X-ray diffraction results [5, 6]. With regard to the three-dimensional structure, the interlayer intercalate ordering is $\alpha, \beta, \gamma, \delta$ for C_8K and α, β, γ for C_8Cs [5, 6]. For the case of C_8K, this stacking corresponds to alternate intercalate layer planes, each containing one of 4 equivalent intercalate positions in the real space unit cell of Fig. 2. For this compound, the carbon layers have AA stacking so that the interlayer structure for C_8K is $A\alpha A\beta A\gamma A\delta$. The three-dimensional structure for C_8Cs is likewise $A\alpha A\beta A\gamma$.

For both the C_8K and C_8Cs structures, the appropriate structure factors can be calculated. The resulting (001) diffraction pattern for C_8Cs is in agreement with the full reciprocal space pattern shown in Fig. 2. The results of Halpin and Jenkins [9] show that the $\alpha, \beta, \gamma, \delta$ stacking leads to the vanishing of all the superlattice electron diffraction spots, such that the pure graphite pattern remains. These authors thus attributed the pure graphite pattern shown in Fig. 1 to certain stage 1

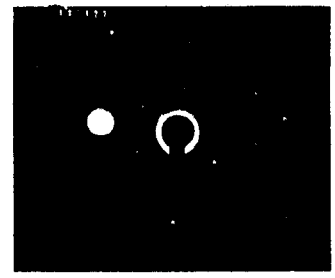

(a)

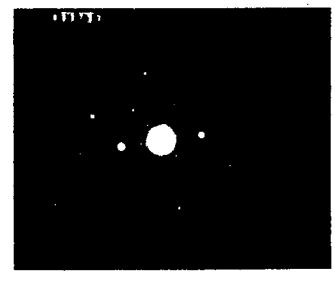

(b)

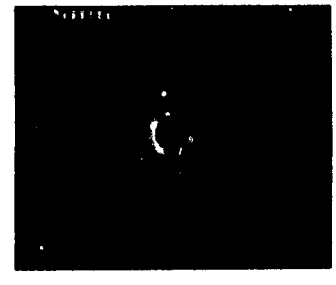

(c)

Fig. 1. Room temperature electron diffraction patterns of: (a) pristine graphite, (b) stage 1 C_8K, (c) stage 1 C_8Cs.

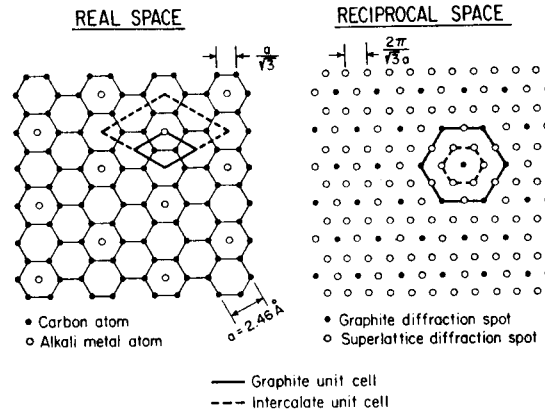

Fig. 2. Intralayer structure for stage 1 C_8X (X = K, Rb, Cs) in real space and reciprocal space.

graphite–alkali metal compounds. These authors did, however, observe the pattern in Fig. 1(b), but attributed this pattern to a "heavily doped" graphite–K compound. We observed the diffraction patterns shown in

Fig. 1(b) and 1(c) for our samples of C_8K and C_8Cs for $77 \lesssim T \lesssim 500$ K, with no evidence for an order–disorder transformation for $T < 500$ K.

We have also investigated the effect of intercalate desorption on the stage 1 graphite–alkali metal compounds, as shown in Fig. 3 for graphite–Cs. Similar effects were observed for graphite–K and graphite–Rb. After slight desorption, a new pattern becomes superimposed on the stage 1 pattern (Fig. 3(b)). After more desorption the stage 1 pattern is completely replaced by this new pattern (Fig. 3(c)). Such patterns for the

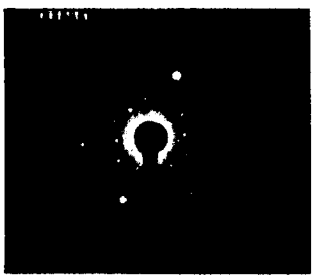

(a)

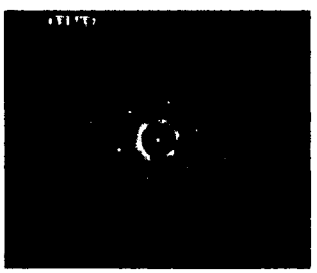

(b)

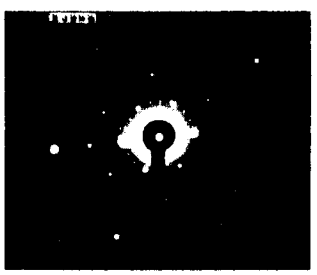

(c)

Fig. 3. Electron diffraction patterns of graphite–Cs after desorption from C_8Cs: (a) stage 1 C_8Cs, (b) after slight desorption, (c) after more desorption.

graphite–alkali metals (K, Rb, and Cs) are shown in Fig. 4, and this is the first reported observation of these electron diffraction patterns. The desorption was carried out for a few minutes or longer in a nitrogen atmosphere at room temperature, and resulted in greyish-blue compounds, typical of high stage graphite–alkali metals. The patterns in Fig. 4 are the most commonly observed patterns in

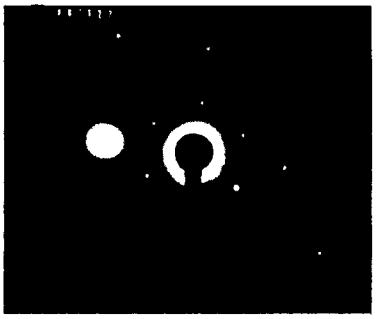

(a)

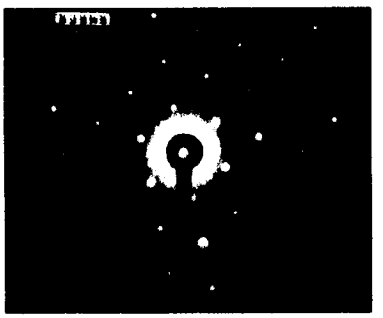

(b)

(c)

(d)

Fig. 4. Liquid nitrogen temperature electron diffraction patterns for graphite–alkali metal compounds after desorption from stage 1 has been completed: (a) pristine graphite, (b) graphite–K, (c) graphite–Rb, (d) graphite–Cs.

our investigation and are interpreted to correspond to the intralayer structure of graphite–alkali metals of stage $\geqslant 2$. The typical patterns for graphite–Rb and graphite–Cs are identical, and are both different from the typical pattern for graphite–K. However, on some portions of our graphite–K samples, the

typical pattern for graphite–Rb (or graphite–Cs) was observed. A possible difference in the intralayer structure of graphite–K from that of graphite–Rb and graphite–Cs has also been reported by Parry *et al.* [8] based on X-ray diffraction intensity data.

These patterns shown in Fig. 4 were obtained with the samples at liquid nitrogen temperature. As the sample temperature is raised, all the superlattice spots disappear, leaving a pure graphite pattern (Fig. 4(a)). This change is reversible on heating and cooling and is interpreted as due to an order–disorder transformation for the intralayer intercalate structure. The transformation temperatures are −63, −4, and 5 °C for graphite–K, graphite–Rb, and graphite–Cs, respectively. Due to possible specimen heating by the electron beam and the limitation in the accuracy of the measurement of the specimen temperature, these transformation temperatures are accurate to ±15 °C. These transformation temperatures are much higher than those previously reported for $C_{24}X$ (X = K, Rb, Cs) on the basis of X-ray diffraction studies [7, 8].

The electron diffraction patterns of Fig. 4 have been interpreted to yield real space unit cells, though the arrangement of the alkali metal atoms within a unit cell has not yet been completely determined [2]. Of significance is the observation that: (1) the real space unit cell is very large for the three patterns shown in Fig. 4(b), (c) and (d); (2) these patterns are *inconsistent* with the simple unit cell (Fig. 5) proposed by Rüdorff and Schulze [5] for the higher stage graphite–alkali metal compounds. The diffraction pattern shown in Fig. 5 has not to our knowledge been observed either by X-ray or electron diffraction techniques. The X-ray diffraction data of Parry *et al.* [8] also do not support this commonly assumed in-plane structure.

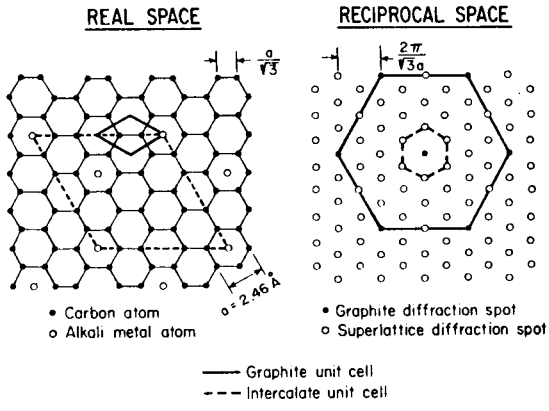

Fig. 5. Intralayer structure for $C_{12}X$ in real space and reciprocal space, as proposed by Rüdorff and Schulze (ref. 5).

To support the contention that the desorption process which results in the patterns in Fig. 4(b), (c), and (d) does not lead to oxidation, we have investigated samples which were deliberately desorbed in air, causing oxidation. The resulting electron diffraction patterns [2] were very different from any reported here.

Because of the finite surface exit resistance of the alkali metals, desorption under vacuum by heating results in the growth of an epitaxial film of alkali metal. The progressive growth of such films has been investigated *in situ* by observing the changes in the electron diffraction pattern as the sample temperature is raised. Figure 6 shows a series of electron dif-

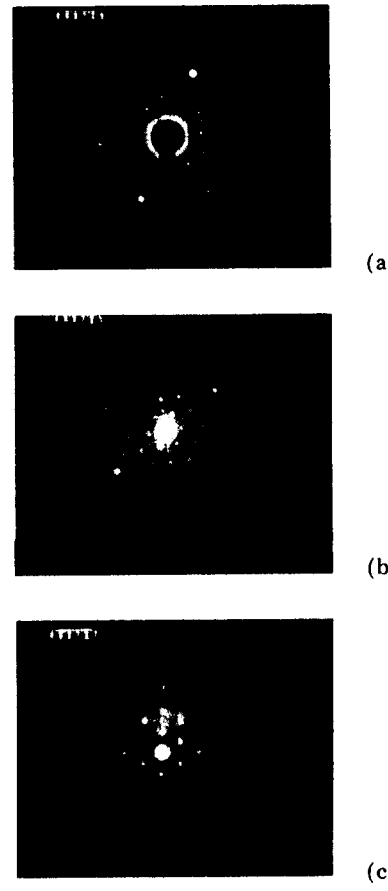

Fig. 6. Electron diffraction patterns of graphite–Cs with epitaxial Cs: (a) C_8Cs, (b) C_8Cs with some epitaxial Cs, (c) epitaxial Cs.

fraction patterns starting with a stage 1 graphite–Cs sample. The same sequence of patterns has been observed for graphite–K. Some desorption occurs at room temperature, so that at room temperature a thin film of epitaxial alkali metal is found on some parts of the sample surface. This results in a superposition of the pattern of the epitaxial metal on the pattern of the stage 1 compound, as shown in Fig. 6(b). As the sample temperature is raised (~200 °C), the desorption rate increases and the epitaxial metal film thickens. On cooling to near room temperature, the epitaxial film remains and gives rise to an electron diffraction pattern (Fig. 6(c)) in which the diffraction spots corresponding to the film replace the spots corresponding to the stage 1 structure. This pattern due to the epitaxial alkali metal film (Fig. 6(c)) has been reported by Halpin and Jenkins [9] for the case of graphite–K, and they also interpreted the pattern in terms of epitaxial metal. The diffraction pattern shown in Fig. 6(c) corresponds to the reciprocal and real space in-plane unit cells shown in Fig. 7. In this case, there is only one

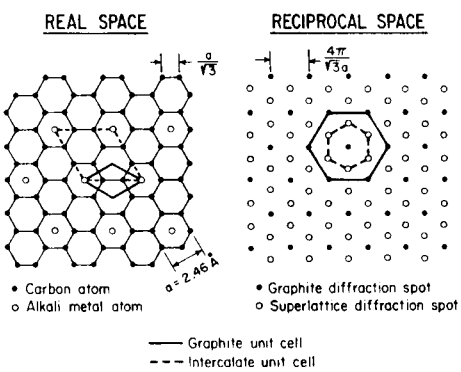

Fig. 7. In-plane structure of an epitaxial alkali metal film on a graphite–alkali metal surface (also C_6X; X = Li) in real space and reciprocal space.

atom per unit cell. This in-plane structure corresponds to the chemical formula C_6X if the material were a stage 1 compound. Such a structure has been found by X-ray diffraction in stage 1 C_6Li [18]. The intercalate density for this structure is higher than that in C_8X. Thus, it appears that the epitaxial alkali metal grows on the graphite substrate in a hexagonal network, similar to the (111) plane of the b.c.c. lattice of the pure alkali metals. It should be emphasized that the unit cell of Fig. 7 is a planar projection of a 3-dimensional structure so that the indicated sites are not necessarily all contained within a single layer plane.

Electron diffraction patterns have also been obtained from lamellar and residue compounds of Br_2, ICl and IBr. Figure 8 shows (001) electron diffraction patterns of pure graphite and several graphite–halogen com-

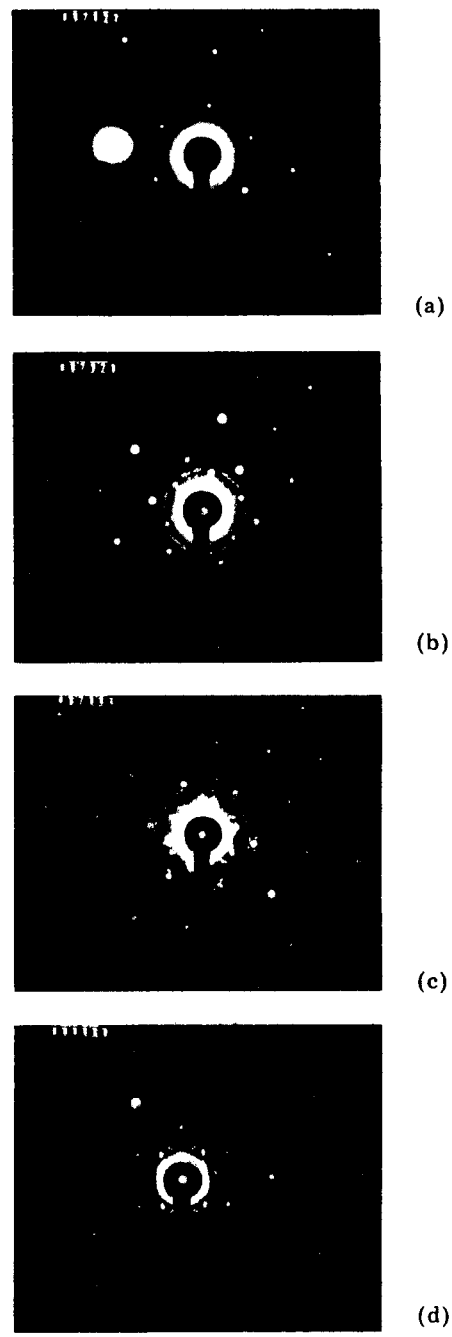

Fig. 8. Room temperature electron diffraction patterns for: (a) pristine graphite, (b) graphite–Br_2, (c) graphite–ICl, (d) graphite–IBr.

pounds at room temperature. For each compound, in addition to the hexagonal pattern of diffraction spots due to graphite, there are superlattice diffraction spots. The superlattice diffraction patterns are different for different intercalates. The patterns for graphite–Br_2 and graphite–ICl have been reported previously by Eeles and Turnbull [10, 11]. The pattern for graphite–IBr is basically similar to that for graphite–ICl, but the relative distances between the various diffraction spots are different for the two interhalogens. The pattern for graphite–Br_2 is significantly different from those for graphite–ICl and graphite–IBr. All the patterns shown in Fig. 8 were taken with the specimen at room temperature. For graphite–ICl and graphite–IBr, the same patterns were observed at all temperatures $77 < T < 300$ K. However, for graphite–Br_2, the diffraction pattern exhibits some changes on lowering the specimen temperature to that of liquid nitrogen, as previously reported by Eeles and Turnbull [10]. In particular, the streaks in the room temperature pattern of Fig. 8 become closely spaced spots in the liquid nitrogen temperature pattern. We have observed this transformation for all the graphite–Br_2 lamellar and residue compounds examined, covering a wide range of concentrations.

Significant changes in the electron diffraction patterns occur on raising the sample temperature above room temperature. For all the graphite–halogens, all the superlattice diffraction spots disappear when a critical sample temperature is reached. Above the critical temperature, which is different for different intercalates, the pattern is the same as that for pure graphite. This change, which is reversible on heating and cooling, is interpreted as an order–disorder transformation for the intralayer intercalate structure. Above the transformation temperature, the intercalate is disordered within each layer. The transformation temperatures are 106, 60 and 43 °C for graphite–Br_2, graphite–IBr, and graphite–ICl, respectively, with an error of ±10 °C. This is the first observation of order–disorder transformations for the intralayer intercalate structure in the graphite–halogens. The change in the graphite–Br_2 pattern from streaks to spots on cooling from 300 to 77 K may be associated with low temperature molecular alignment. Observations of the diffraction patterns as a function of intercalate concentration indicate that the intralayer intercalate structure of graphite–Br_2 does not depend on intercalate concentration, so that an increase in intercalate concentration increases the number of intercalate layers without changing the arrangement of the intercalate within an intercalate layer. Moreover, these observations provide evidence for the presence of intralayer intercalate ordering in dilute lamellar compounds of stages $\gg 5$ and, further, show that intralayer ordering is present in even dilute residue compounds, a point about which there has been some controversy [19].

In addition to the superlattice diffraction pattern due to the intralayer intercalate ordering shown in Fig. 8, another superlattice of hexagonal symmetry was observed in graphite–Br_2 samples. This simple hexagonal superlattice pattern is at an angle of 30° from the graphite pattern and has a periodicity of ~36 Å, which is equal to $\sim 25a_0$ (a_0 = 1.42 Å). Because of the error involved in determining such a large real space periodicity (small reciprocal space periodicity), it is not certain whether the periodicity of this structure is commensurate or incommensurate with the graphite lattice. The patterns observed for both graphite–Br_2 compounds of different intercalate concentrations are essentially identical. The pattern is not observed in pure graphite. This superlattice structure is tentatively identified with the presence of charge-density waves (CDWs).

On heating the graphite–Br_2 sample to ~106 °C, the superlattice pattern (Fig. 8(b)) due to the intralayer intercalate ordering disappears as a result of an order–disorder transformation. However, the other superlattice pattern identified with the CDW remains up to ≈194 °C, at which it also disappears, leaving the pattern for pristine graphite (Fig. 8(a)). The change seems to be reversible, but with large hysteresis. Anomalies in the temperature dependence of the electrical resistivity of graphite–Br_2 have been reported for $200 < T < 400$ °C [20] and may be related to these electron diffraction results. Similar electron diffraction superlattice patterns observed in the layered transition metal dichalcogenides (*e.g.*, 2H $TaSe_2$) [21] have been identified with CDWs. In the case of graphite–halogen intercalation compounds, CDWs could be associated with the ordering

of charged molecular species in a lattice of neutral intercalate molecules.

ACKNOWLEDGEMENT

We would like to thank Prof. J. Vander Sande for many discussions on the interpretation of the electron diffraction patterns and for help with the measurements.

REFERENCES

1 A. W. Moore, in P. L. Walker, Jr. (ed.), Chemistry and Physics of Carbon, 11, Marcel Dekker, New York, 1973, p. 69.
2 D. D. L. Chung, Ph. D. Thesis, Dept. Materials Science and Engineering, Massachusetts Inst. Technol., Cambridge, MA, U.S.A., 1977, unpublished.
3 A. Schleede and M. Wellmann, Z. Phys. Chem., B, 18 (1932) 1.
4 A. Hérold, Bull. Soc. Chim. Fr., 187 (1955) 999.
5 W. Rüdorff and E. Schulze, Z. Anorg. Allg. Chem., 277 (1954) 156.
6 D. E. Nixon and G. S. Parry, Brit. J. Appl. Phys., 1 (1968) 291.
7 G. S. Parry and D. E. Nixon, Nature (London), 216 (1967) 909.
8 G. S. Parry, D. E. Nixon, K. M. Lester and B. C. Levene, J. Phys. C., 2 (1969) 2156.
9 M. K. Halpin and G. M. Jenkins, 3rd Conf. Ind. Carbon and Graphite, Soc. Chem. Ind., London, 1970, p. 53.
10 W. T. Eeles and J. A. Turnbull, Proc. R. Soc. London, Ser. A, 283 (1965) 179.
11 J. A. Turnbull and W. T. Eeles, 2nd Conf. Ind. Carbon and Graphite, 1965, Soc. Chem. Ind., London, 1966, p. 173.
12 J. M. Cowley and J. A. Ibers, Acta Crystallogr., 9 (1956) 421.
13 A. W. Symme Johnson, Acta Crystallogr., 23 (1967) 770.
14 T. Sasa, Y. Takahashi and T. Mukaibo, Carbon, 9 (1971) 407.
15 D. E. Nixon, G. S. Parry and A. R. Ubbelohde, Proc. R. Soc. London, Ser. A, 291 (1966) 324.
16 A. R. Ubbelohde, Proc. R. Soc. London, Ser. A, 304 (1968) 25.
17 D. G. Onn, G. M. T. Foley and J. E. Fischer, Bull. Am. Phys. Soc., 22 (1977) 421; D. G. Onn, G. M. T. Foley and J. E. Fischer, Mater. Sci. Eng., 31 (1977) 271.
18 D. Guérard and A. Hérold, Carbon, 13 (1975) 337.
19 G. R. Hennig, J. Chem. Phys., 20 (1952) 1438.
20 K. Miyauchi, Y. Takahashi and T. Mukaibo, Carbon, 9 (1971) 807.
21 J. A. Wilson, F. J. DiSalvo and S. Mahajan, Adv. Phys., 24 (1975) 117.